

Rotationally Resolved Spectra of Isovalent NbCr and VCr[†]

Shane M. Sickafoose, Jon D. Langenberg, and Michael D. Morse*

Department of Chemistry, University of Utah, Salt Lake City, Utah 84112

Received: September 14, 1999; In Final Form: January 11, 2000

Resonant two-photon ionization spectroscopy has been used to study the isovalent metal molecules NbCr and VCr. The first experimental observation of ⁹³Nb⁵²Cr yielded a ground-state rotational constant of $B''_0 = 0.141\,04(2)\text{ cm}^{-1}$, which corresponds to a bond length of $r''_0 = 1.8940 \pm 0.0003\text{ \AA}$. The excited state, which lies at $14\,440\text{ cm}^{-1}$, has $B'_0 = 0.144\,39(2)\text{ cm}^{-1}$ and $r'_0 = 1.8720 \pm 0.0001\text{ \AA}$. The bond energy of NbCr is measured as $24\,409 \pm 5\text{ cm}^{-1}$ ($3.0263 \pm 0.0006\text{ eV}$) by the onset of predissociation in a congested vibronic spectrum. For ⁵¹V⁵²Cr, the ground state is identified as ² $\Delta_{5/2}$ with $B''_0 = 0.219\,91(26)\text{ cm}^{-1}$ and $r''_0 = 1.7260 \pm 0.0011\text{ \AA}$. The excited state, which lies at $14\,371\text{ cm}^{-1}$, has $B'_0 = 0.221\,53(27)\text{ cm}^{-1}$ and $r'_0 = 1.7201 \pm 0.0011\text{ \AA}$. On the basis of these results, a consistent set of multiple bonding radii are presented for the V, Cr, Nb, and Mo atoms, and the bond lengths (r_0) of VMo and NbMo are predicted to be 1.859 and 2.013 \AA , respectively. A comparison of bond energies for the NbM molecules is also presented, along with an analysis of the trend in bond energies as the metal M is varied.

I. Introduction

Many experimental and theoretical studies have examined the group 5 and group 6 transition metal dimers,^{1–13} characterizing the homonuclear diatomics V₂, Cr₂, Nb₂, and Mo₂, as well as the intragroup heteronuclear diatomics VNb and CrMo. In contrast, rather little is known about the mixed group 5/6 dimers. To our knowledge, only five previous studies exist concerning the mixed group 5/6 dimers. A Knudsen effusion mass spectrometric study by Gupta and Gingerich determined the bond energy for NbMo to be $4.64 \pm 0.26\text{ eV}$ in 1978.¹⁴ Absorption spectra of NbMo isolated in solid argon have also been reported, with several transitions observed in the 550–590-nm region.¹⁵ Density functional theory was employed by Mattar and Doleman to examine VCr, determining its binding energy and spectroscopic constants.¹⁶ More recently, a photoelectron spectroscopic study by Alex and Leopold,¹⁷ in combination with a CASSCF/CASPT2 calculation by Andersson,¹⁸ elucidated much about the low-lying states of VCr. The spectra and measured spectroscopic constants presented here represent the first data of any kind concerning NbCr and provide confirmation of the results of the theoretical treatments of VCr.

II. Experimental Section

Diatomic NbCr and VCr were formed by pulsed-laser ablation (Nd:YAG, 532 nm, 9 mJ per pulse) of alloy disks with mole ratios of 4:1 (Cr:Nb or Cr:V), followed by supersonic expansion in helium carrier gas. After expansion into vacuum, the molecular jet was skimmed, and the collimated supersonic beam was admitted into a second chamber where it was exposed to tunable visible radiation produced by a Nd:YAG pumped dye laser. Photoionization of any excited states so produced was accomplished using the 248-nm radiation produced by an excimer laser operating on a KrF mixture. The ionized molecules were then detected in a reflectron time-of-flight mass spec-

trometer. A complete description of the experimental details has been previously published.¹⁹

The greatest concentrations of the heteronuclear molecules VCr and NbCr that could be produced are estimated to be less than 5% of the concentrations of the homonuclear molecules V₂ and Nb₂, respectively. This is presumably because the high bond energies of V₂ (2.75 eV)²⁰ and Nb₂ [$5.24(13)\text{ eV}$]²¹, as compared to VCr (calculated $D_e = 2.262\text{ eV}$)¹⁸ and NbCr (3.026 eV , see below), facilitated the displacement reactions $V + VCr \rightarrow V_2 + Cr$ and $Nb + NbCr \rightarrow Nb_2 + Cr$, thereby leading to the removal of the target molecules from the molecular beam. To overcome this problem, the samples were enriched in Cr, as described above. Even so, the heteronuclear molecules (⁵¹V⁵²Cr and ⁹³Nb⁵²Cr) showed an extremely weak signal intensity, even when on resonance, compared to the homonuclear signals for V₂ and Nb₂. Because of this weak signal strength, it was impossible to record spectra for any of the minor isotopes of VCr or NbCr, and it was likewise impossible to resolve the hyperfine structure of NbCr.

III. Results

A. VCr. Two transitions of reasonably strong intensity were found in VCr near $14\,000\text{ cm}^{-1}$. Attempts to rotationally resolve the stronger of the two, at $14\,693\text{ cm}^{-1}$, resulted in an unassignable spectrum. This difficulty was probably due to a perturbing state at slightly higher energy. A weaker transition, near $14\,371\text{ cm}^{-1}$, of roughly half the intensity of the $14\,693\text{ cm}^{-1}$ band, proved to be resolvable and assignable, however. The rotationally resolved spectrum is displayed in Figure 1, with the assigned transitions listed in Table 1. The spectrum displays the symmetrical structure of a transition in which B'' and B' are nearly equal; in fact, the Q branch appears degraded neither toward the red nor toward the blue. This observation is verified in the fitted rotational constants, $B''_0 = 0.219\,91(26)\text{ cm}^{-1}$ and $B'_0 = 0.221\,53(27)\text{ cm}^{-1}$, which differ by less than 1%.

These effective rotational constants differ from true mechanical rotational constants as a result of S- and L-uncoupling interactions with other states.²² For the diatomic transition

[†] Part of the special issue "Marilyn Jacox Festschrift".

* E-mail: Michael.Morse@chemistry.utah.edu. Fax: (801)-581-8433.

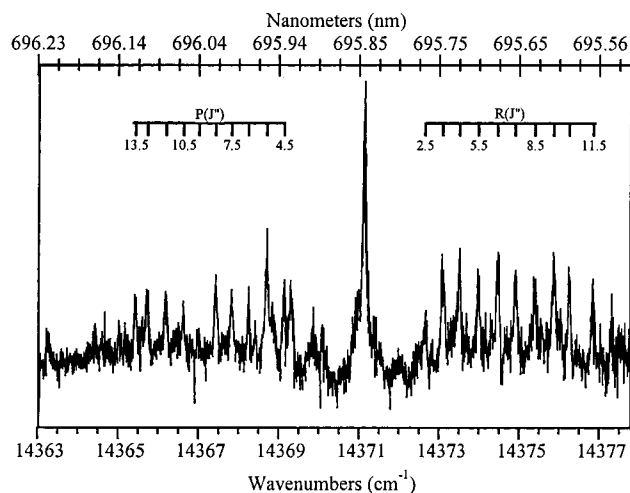


Figure 1. Rotationally resolved scan over the $14\,371\text{ cm}^{-1}$ band of $^{51}\text{V}^{52}\text{Cr}$. From the analysis of this $\Omega' = 5/2 \leftarrow \Omega'' = 5/2$ band, the ground-state bond length of VCr is deduced to be $r_0'' = 1.7260(11)\text{ \AA}$.

metals, these effects are usually small unless the perturbing states lie very close in energy. For the ground state, which is shown in the next paragraph to be a ${}^2\Delta_{5/2}$ state, the obvious perturber is the higher-energy ${}^2\Delta_{3/2}$ spin-orbit component. For such a situation, the true rotational constant, B_{true} , is related to the effective rotational constant, B_{eff} , by the formula²³

$$B_{\text{eff}} = B_{\text{true}} + \frac{2B_{\text{true}}^2 \Sigma}{A\Lambda} \quad (3.1)$$

For the VCr molecule, A is expected to fall between the values of the spin-orbit parameter, $-\zeta_{3d}$, for V and Cr, placing A in the range of -177 to -243 cm^{-1} .²⁴ Thus, the value of B_{true} is slightly modified compared to the fitted value of B''_0 , giving $B''_0(\text{true}) = 0.220\,03(28)\text{ cm}^{-1}$. This value corresponds to a bond length of $r''_0 = 1.7260(11)\text{ \AA}$. Here and throughout this article, we report 1σ error limits in units of the last reported digit in parentheses.

The similar intensities of the R and P branches, along with the relative weakness of the Q branch, for which all of the lines overlap, imply that this is a parallel ($\Delta\Omega = 0$) transition. The observation of R(2.5) as the first R line then identifies the band as an $\Omega' = 2.5 \leftarrow \Omega'' = 2.5$ transition. As such, the first P line should be P(3.5), but this line is not readily identified in the spectrum. A candidate line lies slightly to the blue of the P(4.5) line, but it lies too far to the red to be included in the least-squares fit as P(3.5). The P(3.5) line appears to be displaced approximately 0.234 cm^{-1} from its expected position by a perturbation with another state. Weak, unassigned features near $14\,370\text{ cm}^{-1}$ may be transitions to rotational levels of this perturbing state. Likewise, the R(10.5) and P(12.5) lines, which terminate on the same rotational level of the upper state, are both shifted to lower energy, again indicating a perturbing state lying close in energy. Because of these apparent perturbations, P(3.5), P(12.5), and R(10.5) were omitted from the least-squares fit. Fitted spectroscopic constants are given in Table 1, along with the residuals in the least-squares fit.

An attempt was made to measure the bond energy of VCr by locating a predissociation threshold in a dense manifold of vibronic levels, as has been previously done for a number of diatomic metal molecules.^{4,7,20,25,26} This attempt was unsuccessful because of the weakness of the VCr signal, combined with the large number of V_2 transitions at higher energies. Even under the best conditions for production of VCr, on resonance,

TABLE 1: Assigned Rotational Lines for $^{51}\text{V}^{52}\text{Cr}^a$

rotational line	observed line position ^b
P(4.5)	14 369.138(-27)
P(5.5)	14 368.692(-6)
P(6.5)	14 368.256(8)
P(7.5)	14 367.822(24)
P(8.5)	14 367.423(7)
P(9.5)	14 366.998(20)
P(10.5)	14 366.623(-15)
P(11.5)	14 366.183(20)
P(12.5)	
P(13.5)	14 365.427(-26)
R(2.5)	14 372.658(-29)
R(3.5)	14 373.101(-17)
R(4.5)	14 373.520(22)
R(5.5)	14 373.991(12)
R(6.5)	14 374.478(-11)
R(7.5)	14 374.914(20)
R(8.5)	14 375.404(1)
R(9.5)	14 375.870(9)
R(10.5)	
R(11.5)	14 376.849(-13)

^a All numerical values are given in wavenumbers (cm^{-1}). Residuals in the fit are given in parentheses in units of 0.001 cm^{-1} . ^b Line positions are determined by calibrating the étalon with the known frequencies of the I_2 absorption spectrum. All line positions are corrected by the Doppler shift experienced by $^{51}\text{V}^{52}\text{Cr}$ as it translates toward the radiation source. The errors associated with the observed line positions are obtained by a least-squares fit of the line positions to the formula $\nu = \nu_0 + B'J'(J' + 1) - B''J''(J'' + 1)$. The resulting values of the parameters are $\nu_0 = 14\,371.0648(82)\text{ cm}^{-1}$, $B''_0 = 0.219\,91(26)\text{ cm}^{-1}$, $B'_0 = 0.221\,53(27)\text{ cm}^{-1}$, $r''_0 = 1.7260(11)\text{ \AA}$, and $r'_0 = 1.7201(11)\text{ \AA}$, where the 1σ error limits are given in parentheses, in units of the last digit quoted. In the calculation of r''_0 , the effects of the spin-uncoupling operator, which couples the ${}^2\Delta_{5/2}$ ground state with the ${}^2\Delta_{3/2}$ excited spin-orbit component, have been included, even though this only leads to a minor change in the estimated bond length of 0.0005 \AA .

the V_2^+ ion signal at mass 102 completely obscured any resonant enhancement in the VCr⁺ signal at mass 103.

B. NbCr. A scan of the excitation laser from 12 000 to 18 000 cm^{-1} revealed only one strong transition in NbCr, at $14\,440\text{ cm}^{-1}$. The first attempt to rotationally resolve this transition produced a spectrum without clear rotational lines. The presumed cause of the poor resolution was the hyperfine splitting induced by the large nuclear magnetic moment of ^{93}Nb ($I = 9/2$), 6.167 nuclear magnetons.²⁷ Recognizing that the hyperfine splitting in a Hund's case-(a) or case-(c) molecule decreases with increasing J as $1/J$,^{28,29} we decided that impeding the cooling effects of the supersonic expansion and populating higher rotational levels might produce narrower, recognizable lines. To warm the molecular beam, a 3.5-in.-long extender with an exit orifice of $3/8$ in. (0.95 cm) was affixed to the end of the vaporization block. This modification moved the expansion orifice much closer to the skimmer, reduced the carrier gas pressure at the nozzle orifice, and effectively moved the probe region much closer to the expansion orifice, in units of nozzle diameter. All of these factors contributed to a reduction in the degree of supersonic cooling, as compared to the standard exit orifice diameter of 0.1 cm. The rotationally resolved spectrum recorded with this extender is displayed in Figure 2. The hyperfine broadening of the low- J lines is evident, with lines below R(6.5) and P(9.5) disappearing into a sea of noise.

As was found for VCr, this band displays R and P branches of comparable intensity and has a much weaker Q branch, implying that it is another parallel ($\Delta\Omega = 0$) transition. The lack of assignable lines in the Q branch, combined with our inability to follow the P and R branches down to their first lines,

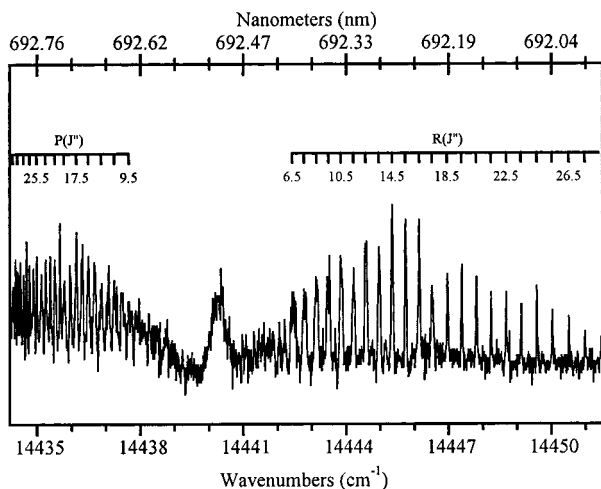


Figure 2. Rotationally resolved scan over the $14\,440\text{ cm}^{-1}$ band of $^{93}\text{Nb}^{52}\text{Cr}$. Although the low- J lines are not resolved because of extensive hyperfine splitting, the analysis of this parallel band provides a value of $r_0'' = 1.8940(3)\text{ \AA}$.

prohibits a definitive experimental assignment of Ω'' and Ω' at this time. It also makes the absolute J -numbering of the lines somewhat problematic. Because the R and P branches lie on the same Fortrat parabola,²² a revised numbering of the branches, in which the R(J) lines are renumbered as R($J + K$) and the P(J) lines are renumbered as P($J - K$), where K is any integer, gives residuals that are precisely identical to those of the original assignment. By simulating the band for various J -numberings and comparing the location of the Q branch to experiment, however, we could make a definitive set of line assignments. The final assignment is given in Table 2, along with the band origin, rotational constants, and bond lengths. The fitted ground-state effective B constant is given by $B''_0 = 0.141\,04(2)\text{ cm}^{-1}$. An analysis of the likely effects of the S-uncoupling operator,²⁴ acting between the presumed $^2\Delta_{5/2}$ ground state and the $^2\Delta_{3/2}$ excited state, leads to an estimated value of $B''_0(\text{true}) = 0.141\,06(4)\text{ cm}^{-1}$. This value corresponds to a ground-state bond length of $r''_0 = 1.8940(3)\text{ \AA}$.

As was done for VCr, an attempt was also made to measure the bond energy of NbCr by locating a sharp predissociation threshold in a dense set of vibronic levels. The lack of other molecules near mass 145 in the mass spectrum allowed this project to succeed despite the small amount of NbCr produced in the molecular beam. The result, displayed in Figure 3, demonstrates a dense set of vibronic levels to the red of $24\,400\text{ cm}^{-1}$ and an abrupt onset of predissociation to the blue of this value. Calibration of the predissociation threshold was accomplished by collecting niobium atomic transitions simultaneously with the threshold and then calibrating the scan over the threshold using the known niobium atomic transitions.³⁰ This provided an assignment of $D_0 = 24\,409 \pm 5\text{ cm}^{-1}$ ($3.0263 \pm 0.0006\text{ eV}$) for the dissociation energy of $^{93}\text{Nb}^{52}\text{Cr}$.

IV. Discussion

A. VCr. The identification of the rotationally analyzed band of VCr as an $\Omega' = 5/2 \leftarrow \Omega'' = 5/2$ transition is consistent with the $^2\Delta_{5/2}$ ground state obtained in previous theoretical investigations.^{16,18} This state arises from a $d\pi^4 d\sigma^2 d\delta^3 s\sigma^2$ configuration in the ab initio calculations of Andersson, where all of the molecular orbitals listed are bonding in character.¹⁸ The bond length of $^{51}\text{V}^{52}\text{Cr}$, $r_0 = 1.7260(11)\text{ \AA}$, is nearly identical to the average (1.731 \AA) of the bond lengths of V_2 [$r_0 = 1.777(5)\text{ \AA}$]¹ and Cr_2 [$r_0 = 1.6858\text{ \AA}$]⁶ and is in good agreement with previous

TABLE 2: Assigned Rotational Lines for $^{93}\text{Nb}^{52}\text{Cr}^a$

rotational line	observed line position ^b	rotational line	observed line position ^b
P(9.5)	14 437.687(9)	R(6.5)	14 442.433(1)
P(10.5)	14 437.488(-11)	R(7.5)	14 442.768(5)
P(11.5)	14 437.268(-3)	R(8.5)	
P(12.5)	14 437.068(-7)	R(9.5)	14 443.468(3)
P(13.5)	14 436.873(-12)	R(10.5)	14 443.841(-11)
P(14.5)	14 436.672(-2)	R(11.5)	14 444.196(0)
P(15.5)	14 436.482(3)	R(12.5)	14 444.565(4)
P(16.5)	14 436.308(-1)	R(13.5)	14 444.948(0)
P(17.5)	14 436.136(-1)	R(14.5)	14 445.331(3)
P(18.5)	14 435.965(5)	R(15.5)	14 445.728(-2)
P(19.5)	14 435.812(0)	R(16.5)	14 446.122(3)
P(20.5)	14 435.654(7)	R(17.5)	14 446.533(-2)
P(21.5)	14 435.518(-2)	R(18.5)	14 446.947(-4)
P(22.5)	14 435.375(2)	R(19.5)	14 447.369(-6)
P(23.5)	14 435.243(3)	R(20.5)	14 447.794(-5)
P(24.5)	14 435.116(5)	R(21.5)	14 448.215(7)
P(25.5)	14 434.991(12)	R(22.5)	14 448.660(1)
P(26.5)	14 434.887(5)	R(23.5)	14 449.096(11)
P(27.5)	14 434.793(-6)	R(24.5)	14 449.559(1)
P(28.5)	14 434.690(0)	R(25.5)	14 450.000(20)
P(29.5)	14 434.600(-2)	R(26.5)	14 450.492(-6)
P(30.5)	14 434.514(-1)	R(27.5)	14 450.964(-5)
P(31.5)	14 434.442(-7)	R(28.5)	14 451.442(-4)
P(32.5)	14 434.367(-3)	R(29.5)	14 451.934(-10)
P(33.5)	14 434.295(5)		
P(34.5)			
P(35.5)	14 434.196(-5)		
P(36.5)	14 434.143(4)		
P(37.5)	14 434.107(2)		
P(38.5)			
P(39.5)	14 434.058(-5)		

^a All numerical values are given in wavenumbers (cm^{-1}). Residuals in the fit are given in parentheses in units of 0.001 cm^{-1} . ^b Line positions are determined by calibrating the étalon with the known frequencies of the I_2 absorption spectrum. All line positions are corrected by the Doppler shift experienced by $^{93}\text{Nb}^{52}\text{Cr}$ as it translates toward the radiation source. The errors associated with the observed line positions are obtained by a least-squares fit of the line positions to the formula $\nu = \nu_0 + B'J'(J' + 1) - B''J''(J'' + 1)$. The resulting values of parameters are $\nu_0 = 14\,440.1052(15)\text{ cm}^{-1}$, $B''_0 = 0.141\,04(2)\text{ cm}^{-1}$, $B'_0 = 0.144\,38(2)\text{ cm}^{-1}$, $r''_0 = 1.8940(3)\text{ \AA}$, and $r'_0 = 1.8720(1)\text{ \AA}$, where the 1σ error limits are given in parentheses, in units of the last digit quoted. In the calculation of r''_0 , the effects of the spin-uncoupling operator, which couples the $^2\Delta_{5/2}$ ground state with the $^2\Delta_{3/2}$ excited spin-orbit component, have been included, even though this only leads to a minor change in the estimated bond length of 0.0001 \AA .

theoretical predictions ($r_e = 1.700\text{ \AA}$ ¹⁶ and $r_e = 1.720\text{ \AA}$ ¹⁸). Previous work on CrMo^9 and VNb^{10} has shown that the bond lengths of these molecules are also nearly equal to the averages of their constituent homonuclear molecules.

A previous photoelectron spectroscopic study by Alex and Leopold,¹⁷ in combination with a CASSCF/CASPT2 calculation by Andersson,¹⁸ has provided considerable insight into the low-lying states of VCr. The $X\ ^2\Delta_i$ ground state is found to have a high vibrational frequency ($\omega_e = 520 \pm 8\text{ cm}^{-1}$, $\omega_e x_e = 7.2 \pm 0.9\text{ cm}^{-1}$ for $^{51}\text{V}^{52}\text{Cr}$),¹⁷ indicating that multiple bonding similar to that found in V_2 and Cr_2 occurs. This is even more apparent in the first excited state observed, which is a $^2\Sigma^+$ state with a leading configuration of $d\pi^4 d\sigma^1 d\delta^4 s\sigma^2$.^{17,18} This $^2\Sigma^+$ state lies at $T_0 = 4485 \pm 15\text{ cm}^{-1}$, with $\omega_e = 715 \pm 11\text{ cm}^{-1}$ and $\omega_e x_e = 12.3 \pm 2.1\text{ cm}^{-1}$. The incredibly high vibrational frequency of this state, along with its low energy, strongly suggests that there is considerable s-d hybridization in VCr,¹⁷ leading to stabilization of one σ orbital and destabilization of the other σ orbital. In a single-configuration wave function, mixing of the $d\sigma$ and $s\sigma$ bonding orbitals has no stabilizing effect on the $d\pi^4 d\sigma^2 d\delta^3 s\sigma^2$, $^2\Delta_i$ ground state, as both orbitals are filled. Such

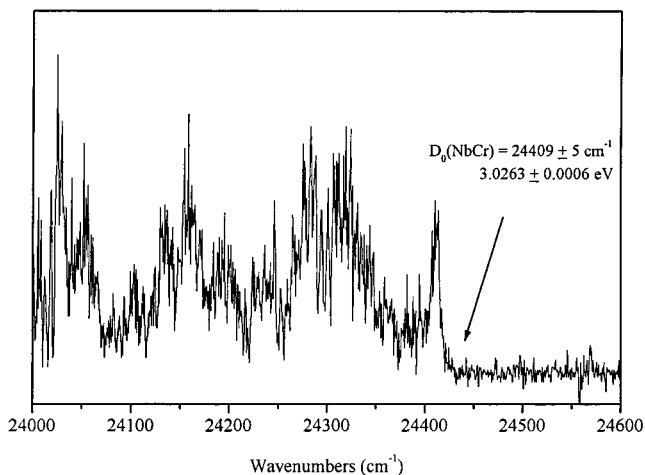


Figure 3. Predissociation threshold of NbCr, observed using resonant two-photon ionization spectroscopy with exalite 411 dye laser radiation for excitation and KrF excimer laser radiation for ionization. The observed predissociation threshold at $24\,409 \pm 5 \text{ cm}^{-1}$ corresponds to a bond energy of $D_0(\text{NbCr}) = 3.0263 \pm 0.0006 \text{ eV}$.

$s-d$ mixing can exert a strong stabilizing influence on states in which these orbitals are only partially filled, however, as in the $d\pi^4 d\sigma^1 d\delta^4 s\sigma^2$, $2\Sigma^+$ state. This has also been found in Ti_2 , where it leads to a $3\Delta_r$ ground state that derives from a $d\pi_u^4 d\sigma_g^2 d\delta_g^1 s\sigma_g^1$ configuration.^{31,32} A similar phenomenon occurs in TiV , which is found to possess a ground electronic state of $d\pi^4 d\sigma^2 d\delta^2 s\sigma^1$, $4\Sigma^-$ in a matrix isolation ESR experiment.³³ Similarly, V_2^+ is now known to have a $d\pi_u^4 d\sigma_g^2 d\delta_g^2 s\sigma_g^1$, $4\Sigma_g^-$ ground state as well.³⁴ In these single-configuration descriptions of the ground electronic states, it should be recognized that the σ orbitals cannot be truly associated with either s - or d -orbital character, because considerable $s-d$ hybridization probably occurs. The designations $s\sigma_g$ and $d\sigma_g$ simply indicate the expected major contributor to these mixed orbitals.

Of greater relevance to the $\Omega = 5/2$ excited state observed in the present study are two 4Δ states of VCr , which were calculated^{17,18} to lie at $T_e = 8293$ and $13\,032 \text{ cm}^{-1}$ and observed¹⁷ at 9220 ± 20 and $12\,160 \pm 20 \text{ cm}^{-1}$, respectively. As calculated by Andersson, these two 4Δ states are strong mixtures of a $d\pi^4 d\sigma^2 d\delta^2 s\sigma^2 d\delta^*1$ and a $d\pi^4 d\sigma^2 d\delta^3 s\sigma^1 s\sigma^*1$ configuration, along with other contributions.¹⁸ These two configurations together generate five 2Δ states, any one of which could correspond to the upper state of our rotationally resolved band. Thus, the electronic transition we observe probably corresponds either to a $\delta^* \leftarrow \delta$ transition (if the upper state derives primarily from $d\pi^4 d\sigma^2 d\delta^2 s\sigma^2 d\delta^*1$) or to a $\sigma^* \leftarrow \sigma$ transition (if the upper state derives primarily from $d\pi^4 d\sigma^2 d\delta^3 s\sigma^1 s\sigma^*1$). The lack of significant hyperfine splitting in the observed spectrum of VCr suggests that the $s\sigma$ orbital remains filled in both the lower and upper states, making it more likely that the observed band corresponds to a $\delta^* \leftarrow \delta$ transition. Otherwise, a significant hyperfine broadening due to the Fermi contact interaction would be expected.^{27,28}

B. NbCr. The rotationally resolved scan displayed in Figure 2 for NbCr has enabled us to make an accurate measurement of the ground-state rotational constant of NbCr, but our inability to assign the low- J region of the spectrum prohibits an absolute assignment of the upper- and lower-state Ω values. Nevertheless, on the basis of the low intensity of the Q branch, the band is clearly a parallel band with $\Delta\Omega = 0$. The only reasonable alternative to the expected $d\pi^4 d\sigma^2 d\delta^3 s\sigma^2$, $2\Delta_i$ ground state is a $d\pi^4 d\sigma^2 d\delta^4 s\sigma^1$ or $d\pi^4 d\sigma^1 d\delta^4 s\sigma^2$, $2\Sigma^+$ ground state similar to the first excited state of VCr , which is found in photoelectron

spectroscopic studies at $4485 \pm 15 \text{ cm}^{-1}$. From a $2\Sigma^+$ state, the only electronic transitions allowed in Hund's case (a) are to another $2\Sigma^+$ state or to a 2Π state. The observed band shows none of the characteristics of these transitions, as a $2\Sigma^+ \leftarrow 2\Sigma^+$ transition would exhibit only R and P branches, corresponding to $\Delta N = \pm 1$, and a $2\Pi \leftarrow 2\Sigma^+$ transition would display four apparent branches for each $2\Pi_{\Omega} \leftarrow 2\Sigma^+$ sub-band.²² Our band clearly displays three branches and, therefore, does not originate from a $2\Sigma^+$ lower state. Although there is no absolute experimental proof that the observed band corresponds to a $2\Delta_{5/2} \leftarrow X\ 2\Delta_{5/2}$ transition, this appears to be the only reasonable alternative.

Our inability to analyze the low- J portion of the spectrum results from the large hyperfine splitting found for the low- J lines. This, too, argues against a $2\Sigma^+$ ground state, because for a Hund's case-(b) $2\Sigma^+$ state, the hyperfine splitting should not decrease as rapidly with increasing J as is observed in our spectrum.²⁸ Indeed, if the spin-rotation constant is small, the hyperfine splitting in a $2\Sigma^+$ state remains nearly constant as N increases, leading to Hund's case-(b) _{β_S} hyperfine coupling,²⁸ as has been observed in ScO ,³⁵ CoC ,³⁶ TiCo ,³⁷ and ZrCo .³⁷ Given that the rotationally resolved band is most likely a $2\Delta_{5/2} \leftarrow X\ 2\Delta_{5/2}$ transition analogous to that observed in VCr , the hyperfine energy in each 2Δ state should follow the expected behavior for a Hund's case-(a) _{β_i} system, for which the hyperfine energy of each state follows the formula

$$E_{\text{hf}}(S, \Lambda, \Sigma, \Omega, I, J, F) = h\Omega \left[\frac{F(F+1) - I(I+1) - J(J+1)}{2J(J+1)} \right] \quad (4.1)$$

to first order in perturbation theory. In this formula, the hyperfine parameter h is given by

$$h = a\Lambda + \left(b_F + \frac{2}{3}c \right) \Sigma \quad (4.2)$$

where

$$a = 2.000 g_I \beta_e \beta_n \langle r^{-3} \rangle \quad (4.3)$$

$$b_F = g_e g_I \beta_e \beta_n \frac{8\pi}{3} |\psi(0)|^2 \quad (4.4)$$

and

$$c = \frac{3}{2} g_e g_I b_e b_n \langle 3 \cos^2 \theta - 1 \rangle \langle r^{-3} \rangle \quad (4.5)$$

Here, $g_e = 2.002\,319\,3$ is the electronic g -factor;²⁷ $g_I \equiv \mu_I/I$ is the nuclear g -factor, given by the nuclear magnetic dipole moment in nuclear magnetons divided by the nuclear spin I ; β_e is the Bohr magneton; β_n is the nuclear magneton; θ is the angle between the internuclear axis and the vector from the magnetic nucleus to the electron; the expectation values provide averages for the single unpaired electron; and $|\psi(0)|^2$ provides the probability density for finding the electron at the magnetic nucleus.²⁷ The numerical factors $g_e \beta_e \beta_n$ combine to give the value $0.003\,186 \text{ cm}^{-1} \cdot \text{bohr}^3$.²⁷

Although it has not been possible for us to analyze the hyperfine structure observed in the spectrum of NbCr because of low signal intensity, the magnitude of the observed splittings is not unreasonable. A range of possible values for the hyperfine constant, h , can readily be predicted using atomic hyperfine parameters for ^{93}Nb . The maximum possible value of the Fermi contact parameter, b_F , can be estimated from the A_{iso} value listed

TABLE 3: Multiple Bonding Radii for V, Cr, Nb, and Mo^a

	V	Cr	Nb	Mo
	0.8896 Å	0.8443 Å	1.0441 Å	0.9718 Å
molecule	measured r_0 (Å)	reference	predicted r_0 (Å) ^b	difference (Å)
V ₂	1.777	1	1.779	-0.002
VNb	1.946	10	1.934	0.012
Nb ₂	2.079	5	2.088	-0.009
VCr	1.726	this work	1.734	-0.007
VMo	unknown		1.861	
NbCr	1.894	this work	1.888	0.006
NbMo	unknown		2.016	
Cr ₂	1.686	6	1.689	-0.003
CrMo	1.823	9	1.816	0.007
Mo ₂	1.940	11	1.944	-0.004

^a The multiple bonding radii were determined by a least-squares fit using the measured bond lengths of the molecules listed here. ^b The predicted values were determined by adding the multiple bonding radii of the constituent atoms.

in Table B1 of Weltner's compilation,²⁷ giving $b_F \leq 0.2198 \text{ cm}^{-1}$. This maximum value could result if the unpaired electron were in an orbital that had purely $5s_{\text{Nb}}$ character, a possibility that is inconsistent with the proposed $d^4d\sigma^2d\delta^3s\sigma^2, ^2\Delta_1$ ground state. On the other hand, the expected values of a and c can also be deduced from the dipolar constants listed in Table B1 of Weltner's book.²⁷ For the proposed $^2\Delta_{5/2}$ ground state, the expected values are $a = 0.015 \text{ cm}^{-1}$ and $c = -0.013 \text{ cm}^{-1}$, giving $h\Omega = 0.065 \text{ cm}^{-1}$. This value is consistent with the observed hyperfine widths, although simulations of the spectrum require that the upper state must then have a value of $h\Omega \approx 0.27 \text{ cm}^{-1}$. This result suggests that the upper state may have some $d^4d\sigma^2d\delta^3s\sigma^1s\sigma^*$, $^2\Delta$ character, allowing a significant Fermi contact interaction (b_F) to develop.

To our knowledge, no previous work, either theoretical or experimental, exists on the NbCr diatomic molecule. Nevertheless, useful comparisons to related molecules can be made. The bond length that was found for NbCr (1.8940 Å) is again remarkably close to the average (1.8826 Å) of the homonuclear molecules Nb₂ ($r_0 = 2.0793 \text{ Å}$)⁵ and Cr₂ ($r_0 = 1.6858 \text{ Å}$).⁶ This result is similar to previous findings comparing the bond lengths of Cr₂, Mo₂, and CrMo and of V₂, Nb₂, and VNb. In fact, if one adopts the multiple bonding radii values of $r(\text{V}) = 0.8896 \text{ Å}$, $r(\text{Cr}) = 0.8443 \text{ Å}$, $r(\text{Nb}) = 1.0441 \text{ Å}$, and $r(\text{Mo}) = 0.9718 \text{ Å}$, the r_0 bond lengths of V₂, Cr₂, Nb₂, Mo₂, VCr, VNb, NbCr, and CrMo are predicted to an accuracy of $\pm 0.012 \text{ Å}$ as the sum of the multiple bonding radii, as shown in Table 3. This demonstrates that the chemical bond is similar in all of these species and allows the bond lengths of the as-yet-unobserved molecules VMo and NbMo to be predicted as $r_0(\text{VMo}) = 1.861 \text{ Å}$ and $r_0(\text{NbMo}) = 2.016 \text{ Å}$.

C. Bond Energies of the NbM and VM Diatomic Metal Compounds. With the measurement of $D_0(\text{NbCr})$ as 3.0263(6) eV, the bond energies of the diatomic compounds of niobium with the 3d transition metals Ti,²⁶ V,⁷ Cr, Co,²⁵ and Ni²⁵ are now accurately known. These energies are listed in Table 4, along with other information about the known or surmised ground states of these molecules. These values allow us to examine the trends in the chemical bonding of the 3d metals with niobium. At first glance, it would appear that the bond energies are fairly uniform, falling within the range of 2.7–3.1 eV for TiNb, NbCr, NbCo, and NbNi. However, VNb severely breaks this uniformity in bond energy with $D_0(\text{VNb}) = 3.789 \text{ eV}$.⁷

Efforts to explain the variation in bond energies among a series of transition metal molecules have, in the past, focused on the concept of promotion energy, which can be loosely defined as the amount of energy required to prepare the transition metal atom for bonding. This concept works reasonably well for the transition metal hydride cations, MH^+ , in which only a single bond can be formed.³⁸ For such molecules, the promotion energy can be defined as the amount of energy required to excite the atom from its ground spin-orbit level to a hypothetical state in which the spin of the s^1 electron that will form the bond is decoupled from that of the remaining d^n electrons.^{38,39} The energy of this spin-decoupled state is taken as the average of the spin-orbit averaged energies of the high-spin and low-spin couplings of the $d^n s^1$ states of the atom. By adding the promotion energy to the measured bond energies, one obtains the bond energy that would be expected if the ground-state atoms were perfectly set up for the formation of an σ bond, such that no promotion energy would be required.

Adapting this concept to the transition metal dimers, we would expect that in cases in which the $s\sigma^*$ orbital is empty in the diatomic ground state, both atoms would require promotion to the spin-uncoupled $d^n s^1$ states prior to bond formation. The other separated-atom limit that can lead to an $s\sigma^2$ bond is the $d^n s^0 + d^m s^2$ asymptote, which is usually much higher in energy for neutral transition metal atoms. Accordingly, we will not consider it further here. On the other hand, for molecules in which the $s\sigma^*$ orbital is singly occupied, only one atom requires promotion prior to bond formation. In the former case, the intrinsic bond energy is given by $D_0(\text{AB}) + P(\text{A}) + P(\text{B})$, whereas for the latter, the intrinsic bond energy is given by $D_0(\text{AB}) + P_{<}(\text{A}, \text{B})$. Here, the promotion energies of atoms A and B are given by $P(\text{A})$ and $P(\text{B})$, and the lesser of these two quantities is given by $P_{<}(\text{A}, \text{B})$. The relevant promotion energies, $P(\text{A})$ and $P(\text{B})$, are listed in Table 4 for the NbM and VM molecules, along with the intrinsic bond energies $D_0(\text{AB}) + P(\text{A}) + P(\text{B})$ or $D_0(\text{AB}) + P_{<}(\text{A}, \text{B})$.

To apply these ideas to the transition metal dimers, we must know how many s-based electrons are present in the molecule. For homonuclear molecules, it is not difficult to count the number of s electrons involved in the bond, at least for examples such as V₂, which has a $[...]4\sigma_g^2 5\sigma_g^2 3\pi_u^4 1\delta_g^2, ^3\Sigma_g^-$ ground state.¹³ In this case, no matter how the $4\sigma_g$ and $5\sigma_g$ orbitals are hybridized, there must be a net total of two $d\sigma$ and two $s\sigma$ electrons, implying that the ground state derives from a $3d^4 4s^1 + 3d^4 4s^1$ separated-atom limit. The situation becomes more problematic in the VNb molecule, where the ground $^3\Sigma^-$ state derives from the $[...]14\sigma^2 15\sigma^2 7\pi^4 2\delta^2$ configuration.⁷ In this case, the lack of inversion symmetry removes the restriction that double occupation of the 14σ and 15σ orbitals must give a net total of two $d\sigma$ and two $s\sigma$ electrons. Nevertheless, it is probably a good approximation to assume that the 14σ and 15σ electrons in VNb correspond to two $d\sigma$ and two $s\sigma$ electrons. This is because of the similar ionization energies of vanadium (IE = 6.746 eV)⁷ and niobium (IE = 6.759 eV),⁴⁰ which imply nearly equal sharing of electrons in the VNb molecule. Thus, the ground state of VNb correlates to a $3d^4 4s^1 + 4d^4 5s^1$ separated-atom limit in which both vanadium and niobium are promoted. More problematic still are the molecules that have an odd number of valence σ electrons, such as TiNb and NbNi, which have ground states of $[...]14\sigma^2 7\pi^4 15\sigma^1 2\delta^2, ^4\Sigma^-$ ⁴¹ and $[...]14\sigma^2 7\pi^4 15\sigma^2 2\delta^4 3\delta^2 16\sigma^1, ^4\Sigma^-$,⁴² respectively. In these cases, the extent of s-d hybridization strongly affects the net number of $s\sigma$ and $d\sigma$ electrons that are assigned to the molecule. Finally, an additional significant problem in using promotion energies

TABLE 4: Bond Energies of NbM and VM Molecules, where M Is a 3d-Series Transition Metal

number of d + s electrons	diatomic molecule	D_0 (eV)	$P(A)$ (eV) ^a	$P(B)$ (eV) ^a	$D_0 + P_{<}$ (eV)	$D_0 + P(A) + P(B)$ (eV)	ground state ^b	references
9	TiNb	3.092(1)	1.113	0.524	3.616	4.729(1)	$7\pi^4 15\sigma^1 2\delta^2, ^4\Sigma^-$	26, 41
10	VNb	3.789(1)	0.636	0.524	4.313	4.949(1)	$7\pi^4 15\sigma^2 2\delta^2, ^3\Sigma^-$	7, 10
11	NbCr	3.0263(6)	0.524	0.471	3.497	4.021(1)	$[7\pi^4 15\sigma^2 2\delta^3, ^2\Delta_i]$	this work
14	NbCo	2.729(1)	0.524	0.648	3.253	3.901(1)	$[7\pi^4 15\sigma^2 2\delta^4 3\delta^1 16\sigma^1, ^3\Delta_r]$	25
15	NbNi	2.780(1)	0.524	0.166	2.946	3.470(1)	$7\pi^4 15\sigma^2 2\delta^4 3\delta^2 16\sigma^1, ^4\Sigma^-$	25, 42
9	TiV	2.068(1)	1.113	0.636	2.704	3.817	$5\pi^4 12\sigma^1 1\delta^2, ^4\Sigma^-$	20, 33
10	V ₂	2.753(1)	0.636	0.636	3.389	4.025	$5\pi^4 12\sigma^2 1\delta^2, ^3\Sigma^-$	1, 3, 20
11	VCr		0.636	0.471			$5\pi^4 12\sigma^2 1\delta^3, ^2\Delta_i$	this work
15	VNi	2.100(1)	0.636	0.166	2.266	2.902(1)	$5\pi^4 12\sigma^2 1\delta^4 2\delta^2 13\sigma^1, ^2\Sigma^+$	20, 33

^a Calculated from the atomic energy levels listed in ref 30. The quantities $D_0 + P_{<}$ and $D_0 + P(A) + P(B)$ represent the intrinsic bond energies that apply for the cases of a diatomic molecule correlating to a $d^n s^1 + d^m s^2$ separated-atom limit and to a $d^n s^1 + d^m s^1$ separated-atom limit, respectively.

^b Ground states listed in square brackets are not known from experimental measurements or ab initio calculations, but represent reasonable guesses based on the known ground states of similar molecules.

to rationalize the measured bond energies of the diatomic transition metal compounds is that, in many cases, the ground electronic state is unknown.

Having noted these caveats, it nevertheless makes sense in the NbM molecules, where M is a 3d metal, to consider the 14σ orbital to be mainly of $5s_{\text{Nb}} + 4s_{\text{M}}$ bonding character and the 15σ orbital to be mainly of $4d_{\text{Nb}} + 3d_{\text{M}}$ bonding character, at least in the early transition metal dimers such as TiNb. In combinations involving the late transition metals, such as NbNi, the compositions of these two σ orbitals can reverse, because of the drop in energy of the d-based orbitals as the nuclear charge of M is increased. Nevertheless, the 16σ orbital, which is nominally antibonding, can be considered to be primarily of s character because, in molecules of this sort, this orbital is so diffuse that it is more appropriately considered nonbonding. This lowers its energy compared to the $d\sigma^*$ orbital, which is strongly antibonding. With these thoughts in mind, it makes sense to consider the TiNb, VNb, and NbCr molecules as correlating to $d^n s^1 + d^m s^1$ separated-atom limits, whereas the NbCo and NbNi molecules, in which the 16σ orbital is presumed or known to be singly occupied, presumably correlate to $d^n s^1 + d^m s^2$ separated-atom limits.

The intrinsic bond energies adopted in Table 4 assume that both transition metal atoms are promoted to $d^n s^1 + d^m s^1$ separated-atom limits for the cases of TiNb, VNb, NbCr, TiV, and V₂, whereas only a single atom is promoted in the cases of NbCo, NbNi, and VNi. The resulting values are given in bold type under the heading of $D_0(\text{AB}) + P(A) + P(B)$ or $D_0(\text{AB}) + P_{<}(\text{A}, \text{B})$, as appropriate. In comparing the intrinsic bond energies of the TiNb, VNb, and NbCr molecules, one should note that these values form a more understandable pattern than do the directly measured dissociation energies, D_0 . Whereas $D_0(\text{VNb})$ is anomalously high compared to both $D_0(\text{TiNb})$ and $D_0(\text{NbCr})$, the intrinsic bond energies of these molecules show TiNb and VNb to have similar bond energies, while a continuous drop in intrinsic bond energies commences with NbCr. Thus, the chemical bonding is similar in TiNb and VNb, except for the extra promotion energy required to prepare Ti for bonding. The same conclusion is also found when comparing the 3d–3d dimers that are isovalent to these molecules, TiV and V₂. In fact, the difference between the intrinsic bond energies of VNb and TiNb, 0.220 eV, almost exactly equals the corresponding difference between V₂ and TiV, 0.208 eV.

The large drop in intrinsic bond energy that is observed in going from VNb to NbCr probably also appears in a comparison of V₂ to VCr. Unfortunately, our lack of a reliable value of $D_0(\text{VCr})$ prohibits a definitive statement on this point. However, a comparison of the intrinsic bond energies of V₂ [$D_0(\text{V}_2) =$

2.753 eV]²⁰ and Cr₂ [$D_0(\text{Cr}_2) = 1.53(6)$ eV],⁴ which are 4.025 and 2.47 eV, respectively, shows a drop of 1.55 eV. This difference compares to a drop in intrinsic bond energy of 0.928 eV when a single V is changed to Cr in moving from VNb to NbCr. Thus, one might expect a similar decrement of 0.77–0.93 eV in moving from V₂ to VCr. This allows the VCr bond energy to be predicted to lie in the range of $1.99 \text{ eV} \leq D_0(\text{VCr}) \leq 2.15 \text{ eV}$. This result compares very well with the bond energy calculated by Andersson, $D_0(\text{VCr}) = 2.062 \text{ eV}$.¹⁸ The significant drop in intrinsic bond energy that is found in going from VNb to NbCr (0.928 eV), or from V₂ to Cr₂ (1.55 eV), probably results from the 10% drop in 3d orbital size in going from V ($\langle r \rangle_{3d} = 0.805 \text{ \AA}$) to Cr ($\langle r \rangle_{3d} = 0.724 \text{ \AA}$),⁴³ along with the concomitant reduction in 3d orbital contributions to the bond.

The continued drop in intrinsic bond energies as one moves from NbCr to NbCo and NbNi reflects the decreasing size of the 3d orbitals as one moves across the 3d series, along with the decreasing involvement of these orbitals in the chemical bond. An additional contributor to the drop in bond energy is the occupation of the nominally antibonding 3δ and 16σ orbitals in the later members of this series of molecules. The occupation of the 16σ orbital is balanced to some degree by the fact that only a single transition metal atom requires promotion to the $d^n s^1$ configuration, however. In going from VNb to NbNi, this drop in intrinsic bond energy amounts to 2.003 eV. Similarly, in the isovalent series of 3d diatomic metal compounds, the intrinsic bond energy drops by 1.759 eV in moving from V₂ to VNi. Although the magnitudes of these reductions in intrinsic bond energy are comparable, they become more nearly equal when expressed as percentages of the total bond energy. The intrinsic bond energy drops by 40.5% in moving from VNb to NbNi; it drops by 43.7% in moving from V₂ to VNi.

V. Conclusion

The ground-state r_0 bond lengths of VCr and NbCr, 1.7260-(11) and 1.8940(3) Å, respectively, have been determined using rotationally resolved optical spectroscopy. These values are in close agreement with available theoretical predictions for VCr and are close to the averages of the r_0 bond lengths of the corresponding homonuclear molecules. On the basis of the known r_0 bond lengths of V₂, Cr₂, Nb₂, Mo₂, VNb, CrMo, and now VCr and NbCr, multiple bonding radii are assigned for the intermetallic bonds of the constituent atoms. These radii reproduce the known bond lengths to an accuracy of 0.012 Å and allow the bond lengths of the as-yet-unmeasured species VMo and NbMo to be predicted as 1.861 and 2.016 Å, respectively. The ground state of VCr is assigned as $^2\Delta_i$, and

the ground state of NbCr is thought to be $^2\Delta_i$ as well, although further experimental work will be required to prove this. The bond energy of NbCr has also been measured to be $24\,409 \pm 5\text{ cm}^{-1}$ ($3.0263 \pm 0.0006\text{ eV}$) by the observation of a sharp predissociation threshold in a dense vibronic spectrum. Finally, the trends in the accurately known bond energies of TiNb, VNb, NbCr, NbCo, and NbNi, along with the isovalent molecules TiV, V₂, and VNi, are discussed.

Acknowledgment. We thank the National Science Foundation for support of this research under Grant CHE-9626557. Acknowledgment is also made to the donors of the Petroleum Research Fund, administered by the American Chemical Society, for partial support of this work.

References and Notes

- (1) Langridge-Smith, P. R. R.; Morse, M. D.; Hansen, G. P.; Smalley, R. E.; Merer, A. J. *J. Chem. Phys.* **1984**, *80*, 593.
- (2) Spain, E. M.; Morse, M. D. *Int. J. Mass Spectrom. Ion Processes* **1990**, *102*, 183.
- (3) Spain, E. M.; Behm, J. M.; Morse, M. D. *J. Chem. Phys.* **1992**, *96*, 2511.
- (4) Simard, B.; Lebeault-Dorget, M.-A.; Marijnissen, A.; ter Meulen, J. J. *J. Chem. Phys.* **1998**, *108*, 9668.
- (5) James, A. M.; Kowalczyk, P.; Fournier, R.; Simard, B. *J. Chem. Phys.* **1993**, *99*, 8504.
- (6) Bondybey, V. E.; English, J. H. *Chem. Phys. Lett.* **1982**, *94*, 443.
- (7) James, A. M.; Kowalczyk, P.; Langlois, E.; Campbell, M. D.; Ogawa, A.; Simard, B. *J. Chem. Phys.* **1994**, *101*, 4485.
- (8) Efremov, Y. M.; Samoilova, A. N.; Gurvich, L. V. *Chem. Phys. Lett.* **1976**, *44*, 108.
- (9) Spain, E. M.; Behm, J. M.; Morse, M. D. *Chem. Phys. Lett.* **1991**, *179*, 411.
- (10) James, A. M.; Kowalczyk, P.; Simard, B. *Chem. Phys. Lett.* **1993**, *216*, 512.
- (11) Hopkins, J. B.; Langridge-Smith, P. R. R.; Morse, M. D.; Smalley, R. E. *J. Chem. Phys.* **1983**, *78*, 1627.
- (12) Efremov, Y. M.; Samoilova, A. N.; Kozhukhovskiy, V. B.; Gurvich, L. V. *J. Mol. Spectrosc.* **1978**, *73*, 430.
- (13) Michalopoulos, D. L.; Geusic, M. E.; Hansen, S. G.; Powers, D. E.; Smalley, R. E. *J. Phys. Chem.* **1982**, *86*, 3914.
- (14) Gupta, S. K.; Gingerich, K. A. *J. Chem. Phys.* **1978**, *69*, 4318.
- (15) Klotzbücher, W. E.; Ozin, G. A. *Inorg. Chem.* **1980**, *19*, 2848.
- (16) Mattar, S. M.; Doleman, B. J. *J. Phys. Chem.* **1994**, *98*, 9764.
- (17) Alex, S. Negative Ion Photoelectron Spectroscopy of Small Transition Metal Clusters. Ph.D. Thesis, University of Minnesota, Minneapolis, MN, 1997.
- (18) Andersson, K., Lund University, Sweden. CASSCF/CASPT2 calculations on VCr, personal communication, May 1996.
- (19) Fu, Z.; Lemire, G. W.; Hamrick, Y. M.; Taylor, S.; Shui, J.-C.; Morse, M. D. *J. Chem. Phys.* **1988**, *88*, 3524.
- (20) Spain, E. M.; Morse, M. D. *J. Phys. Chem.* **1992**, *96*, 2479.
- (21) Hales, D. A.; Lian, L.; Armentrout, P. B. *Int. J. Mass Spectrom. Ion Processes* **1990**, *102*, 269.
- (22) Herzberg, G. *Molecular Spectra and Molecular Structure I. Spectra of Diatomic Molecules*, 2nd ed.; Van Nostrand Reinhold: New York, 1950.
- (23) Adam, A. G.; Azuma, Y.; Barry, J. A.; Huang, G.; Lyne, M. P. J.; Merer, A. J.; Schröder, J. O. *J. Chem. Phys.* **1987**, *86*, 5231.
- (24) Lefebvre-Brion, H.; Field, R. W. *Perturbations in the Spectra of Diatomic Molecules*; Academic Press: Orlando, FL, 1986.
- (25) Arrington, C. A.; Blume, T.; Morse, M. D.; Doverstål, M.; Sassenberg, U. *J. Phys. Chem.* **1994**, *98*, 1398.
- (26) Langenberg, J. D.; Morse, M. D. *Chem. Phys. Lett.* **1995**, *239*, 24.
- (27) Weltner, W., Jr. *Magnetic Atoms and Molecules*; Dover Publications: New York, 1983.
- (28) Dunn, T. M. Nuclear Hyperfine Structure in the Electronic Spectra of Diatomic Molecules. In *Molecular Spectroscopy: Modern Research*; Rao, K. N., Mathews, C. W., Eds.; Academic Press: New York, 1972; p 231.
- (29) Frosch, R. A.; Foley, H. M. *Phys. Rev.* **1952**, *88*, 1337.
- (30) Moore, C. E. *Atomic Energy Levels*; U.S. Circ. No. 467 ed.; National Bureau of Standards, U.S. Government Printing Office: Washington, DC, 1971.
- (31) Doverstål, M.; Lindgren, B.; Sassenberg, U.; Arrington, C. A.; Morse, M. D. *J. Chem. Phys.* **1992**, *97*, 7087.
- (32) Bauschlicher, J. C. W.; Partridge, H.; Langhoff, S. R.; Rosi, M. J. *Chem. Phys.* **1991**, *95*, 1057.
- (33) Van Zee, R. J.; Weltner, J. W. *Chem. Phys. Lett.* **1984**, *107*, 173.
- (34) Yang, D. S.; James, A. M.; Rayner, D. M.; Hackett, P. A. *J. Chem. Phys.* **1995**, *102*, 3129.
- (35) Adams, A.; Klempner, W.; Dunn, T. M. *Can. J. Phys.* **1968**, *46*, 2213.
- (36) Barnes, M.; Merer, A. J.; Metha, G. F. *J. Chem. Phys.* **1995**, *103*, 8360.
- (37) Sickafoose, S. M.; Hales, D. A.; Morse, M. D. In preparation.
- (38) Elkind, J. L.; Armentrout, P. B. *Inorg. Chem.* **1986**, *25*, 1078.
- (39) Mandich, M. L.; Halle, L. F.; Beauchamp, J. L. *J. Am. Chem. Soc.* **1984**, *106*, 4403.
- (40) Rayner, D. M.; Mitchell, S. A.; Bourne, O. L.; Hackett, P. A. *J. Opt. Soc. Am. B* **1987**, *4*, 900.
- (41) Van Zee, R. J.; Li, S.; Weltner, W., Jr. *J. Chem. Phys.* **1995**, *103*, 2762.
- (42) Cheeseman, M.; Van Zee, R. J.; Weltner, W., Jr. *High Temp. Sci.* **1988**, *25*, 143.
- (43) Fischer, C. F. *The Hartree-Fock Method for Atoms*; John Wiley & Sons: New York, 1977.